Photoinduced Nonadiabatic Dynamics of Pyrimidine Nucleobases: On-the-Fly Surface-Hopping Study with Semiempirical Methods

3 AUTHORS, INCLUDING:

Lan Zhenggang

Qingdao Institute of Bioenergy and Biopro…

58 PUBLICATIONS **1,159** CITATIONS

SEE PROFILE

Eduardo Fabiano

Italian National Research Council

76 PUBLICATIONS **1,221** CITATIONS

SEE PROFILE

Article

Photoinduced Nonadiabatic Dynamics of Pyrimidine Nucleobases: On-the-Fly Surface-Hopping Study with Semiempirical Methods

Zhenggang Lan, Eduardo Fabiano, and Walter Thiel

More About This Article

Additional resources and features associated with this article are available within the HTML version:

- Supporting Information
- Access to high resolution figures
- Links to articles and content related to this article
- Copyright permission to reproduce figures and/or text from this article
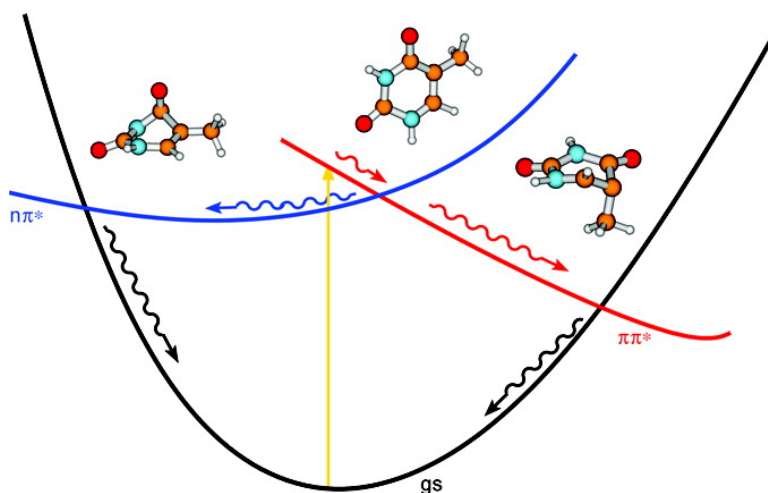
View the Full Text HTML

Photoinduced Nonadiabatic Dynamics of Pyrimidine Nucleobases: On-the-Fly Surface-Hopping Study with Semiempirical Methods

Zhenggang Lan,* Eduardo Fabiano, and Walter Thiel

Max-Planck-Institut für Kohlenforschung, Kaiser-Wilhelm-Platz 1, D-45470, Mülheim an der Ruhr, Germany

*Received: October 14, 2008; Revised Manuscript Received: January 6, 2009*

The photoinduced relaxation dynamics of pyrimidine nucleobases (uracil, thymine, and cytosine) was studied using the surface-hopping approach at the semiempirical OM2/MRCI level of theory. The relevant potential energy surfaces were characterized by performing geometry optimizations of the energy minima of the lowest electronic states and of the most important conical intersections and by computing excitation energies at each configuration. Surface-hopping molecular dynamics simulations were performed to describe the nonadiabatic dynamics after excitation into the optically active state. In each of the molecules, the two lowest excited singlet states are involved in the dynamics, and there are competing relaxation paths. The dynamics is dominated by a two-step relaxation mechanism in uracil and thymine, while the direct decay to the ground state is most important in cytosine. For all three molecules, the simulations yield ultrafast S_2-S_1 deexcitation within 50 fs and internal conversion to the ground state in less than 1 ps, consistent with recent experimental results from time-resolved photoelectron spectroscopy.

Introduction

The study of the photophysical and photochemical behavior of electronically excited states of nucleic acid bases[1-4] is fundamental to understanding the resistance of genetic material to UV-induced damage. DNA and RNA bases absorb strongly in the UV range but photoisomerization and subsequent photodegradation are rarely observed since the excess energy is efficiently dissipated through nonradiative decay channels and transferred to the environment. This photostability is extremely important to preserve the genetic information stored in DNA chains.

The pyrimidine bases uracil, thymine, and cytosine are the simplest nucleobases. They have been often used as prototypes to investigate the photostability of DNA and RNA bases.[1-36] In their electronic spectra, there is a broad absorption band centered at 4-6 eV,[4] assigned to the transition between the ground state (gs) and a $\pi\pi^*$ state. In the same energy range, circular dichroism spectra reveal the presence of a dark excited-state of $n\pi^*$ character.[4] The broadness of the absorption band is often interpreted as indicative of the short lifetime of the $\pi\pi^*$ state.[2,3] Indeed, recent time-resolved photoelectron spectroscopy studies report for each of the pyrimidine nucleobases a double exponential decay comprised of an ultrafast component with a lifetime below 50 fs and a second component with a lifetime in the subpicosecond regime.[3,18] The very short decay times suggest that the electronic relaxation proceeds by nonadiabatic dynamics in the singlet manifold, through internal conversion via the corresponding conical intersections.

Several conical intersections between the three lowest singlet states of pyrimidine bases have been located in ab initio[2-6,10,11,16,17,20,21,26,27,29,34,36] and density functional theory (DFT) studies.[2,7,19,22,24] In uracil and thymine, the $\pi\pi^*$ state and the ground state are connected by a conical intersection characterized by a strong out-of-plane distortion at the C5 atom site[17,20,24,26,27,36] (for atom labeling see Figure 1), while a strong
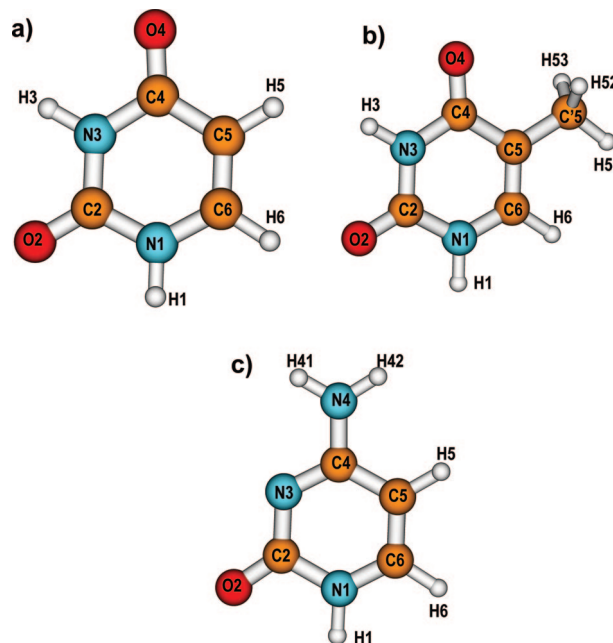
Figure 1. Molecular structures and atom numbering of uracil (a), thymine (b), and cytosine (c).

out-of-plane distortion at the O4 atom leads to a conical intersection between the $n\pi^*$ and the ground state.[17,20,26,36] In cytosine, there are similar conical intersections.[2,10,11,16,19,27,29] Moreover, all three molecules have a conical intersection connecting the $\pi\pi^*$ state and the $n\pi^*$ state[10,11,16,17,19,20,24,26,27,29,34] that is characterized by rather small geometrical distortions and lies close to the Franck-Condon region.

On the basis of theoretical calculations and experimental evidence, several possible mechanisms have been proposed for the nonradiative deexcitation of the pyrimidine bases. The existence of a conical intersection between the optically active $\pi\pi^*$ state and the ground state has often been used to suggest that the nonradiative relaxation proceeds through a direct $\pi\pi^*$

* To whom correspondence should be addressed. E-mail: lan@mpi-muelheim.mpg.de.

→ gs decay.[2,3,17,20,24,26,27,29] Alternatively, a two-step deexcitation, involving a $\pi\pi^* \rightarrow n\pi^* \rightarrow$ gs path, has been proposed by some authors,[2,3,16,32,35] at least for those systems (i.e., uracil and thymine) where the $\pi\pi^*$ state is higher than the $n\pi^*$ state in the Franck–Condon region. In the case of uracil, the excited-state decay has been interpreted in terms of a direct $\pi\pi^* \rightarrow$ gs path and a slower indirect $\pi\pi^* \rightarrow n\pi^* \rightarrow$ gs path (with trapping in and recrossing from the $n\pi^*$ minimum).[34] Finally, for high excitation energies, a decay mechanism has been considered that involves Rydberg-type $\pi\sigma^*$ states which cross the $\pi\pi^*$ and the ground-state potential energy surfaces along a hydrogen-detachment reaction coordinate.[18,37]

Experimentally, the decay times of excited states of pyrimidine bases have recently been measured with high accuracy,[3,18] but the different decay mechanisms could not be identified precisely. On the other hand, theory can provide detailed information on existing conical intersections and possible decay paths. However, most published theoretical studies either lack a dynamical treatment or only include a few degrees of freedom and therefore have not been able to determine the relative importance of different relaxation pathways and to predict the different decay times. These limitations have been overcome by a recent ab initio multiple spawning (AIMS) study of nonadiabatic dynamics in uracil and thymine[30,31] that directly simulated their time-resolved photoelectron spectra by computing the total photoionization probability at the CASSCF level; on the basis of 500 fs AIMS simulations, the ultrafast decay of the photoelectron signal was attributed to the relaxation to a true minimum on the S_2 potential energy surface and not to electronic quenching as in previous work. It should be noted that the existence of such an S_2 minimum has not yet been firmly established since the commonly found CASSCF minimum tends to disappear when applying higher-level ab initio methods or unconstrained optimization.[17,26,27,34] Further dynamics studies thus appear desirable for a detailed mechanistic understanding of photoinduced nonradiative relaxation in the pyrimidine bases.

In this article, we follow the approach used in our previous work on the nonadiabatic dynamics of adenine[38] and study the photoinduced relaxation of pyrimidine bases using on-the-fly surface-hopping molecular dynamics simulations. The potential energy surfaces and nonadiabatic coupling vectors are calculated on-the-fly using the OM2 semiempirical Hamiltonian[39,40] and GUGA multireference configuration interaction (GUGA-CI).[41] The hopping probabilities are computed using the fewest-switches algorithm.[42,43] This provides an efficient description of the relaxation dynamics of the pyrimidine bases and allows us to assess the role of different decay mechanisms and to obtain decay times in good agreement with experimental measurements.

Computational Details

All calculations were performed using the semiempirical MNDO program.[44] The orthogonalization-corrected OM2 semiempirical Hamiltonian[39,40] and the GUGA-CI approach[41] were employed to calculate the required energies, gradients, and nonadiabatic coupling vectors. In GUGA-CI calculations, three reference configurations were used (closed-shell, single, and double HOMO–LUMO excitations), and the active space was chosen to include three occupied π orbitals, one occupied n orbital and three unoccupied π^* orbitals with eight electrons in seven molecular orbitals. Calculations on uracil and thymine were performed using the open-shell SCF approach, while the closed-shell SCF approach was used for cytosine.

For all molecules, the equilibrium geometries of the ground state and of the lowest excited singlet states were optimized,

and the conical intersections connecting these electronic states were located using a Lagrange–Newton method.[45,46] Excitation energies were calculated at each optimized geometry. Only the two lowest excited singlet states were considered in these calculations, since these are the only ones involved in the relaxation dynamics. It should be noted that excited states of $\pi\sigma^*$ character are excluded in the present study because their Rydberg-type character cannot be correctly described by the semiempirical OM2 approach. However, the contribution of these states to the nonadiabatic dynamics of DNA bases is believed to be important only for either relatively high or low excitation energies.[47,48] For this reason, they are neglected in the present calculations, which focus on excitations in the middle of the absorption band (see sampling procedure below).

The photoinduced nonadiabatic dynamics was studied by on-the-fly surface-hopping simulations, performed using the recent surface-hopping MNDO implementation.[49] The initial configurations were sampled by applying the selection criterion described in refs 49 and 50 to a large number of geometries obtained from a preliminary ground-state molecular dynamics simulation. In this way, a reliable sampling of the center of the absorption band is performed.[38,50] Nuclear degrees of freedom were propagated along classical trajectories for 1.6 ps with a time step of 0.1 fs, using the velocity-Verlet algorithm.[51] The time evolution of quantum amplitudes along the trajectories was calculated using a unitary propagator and a time step 200 times smaller. The hopping probabilities were computed by the fewest switches algorithm.[42,43] The adiabatic representation was used in all calculations. Final results were obtained by averaging over 105, 96, and 126 trajectories for uracil, thymine, and cytosine, respectively. Further technical details about the surface hopping calculations are documented in refs 38 and 49.
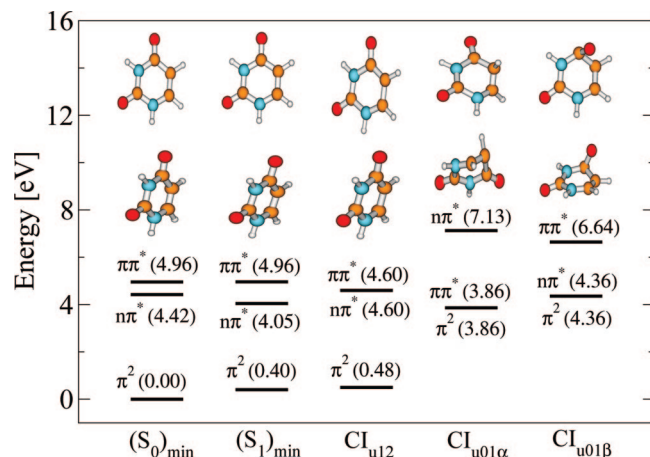
Results

In this section, we present the results of calculations on uracil, thymine, and cytosine (see Figure 1 for atom numbering). We report for each molecule the main features of the potential energy surfaces and the nonadiabatic dynamics. Detailed numerical results for the optimized geometries of energy minima and conical intersections and for the excitation energies at these optimized geometries are given in the Supporting Information (Tables S1–S21). The nonadiabatic dynamics can be analyzed in terms of the time-dependent occupations of the adiabatic states that are also shown in the Supporting Information (Figures S1–S3). Decay mechanisms and paths are identified by inspection of the individual surface-hopping trajectories and determination of the electronic character of states involved in the dynamics.

The nonadiabatic dynamics from surface-hopping simulations can be related to the results from time-resolved photoelectron spectroscopy (TRPES) experiments.[18] A strict comparison of computed decay times with experimental time constants is not possible since our calculations are performed in the adiabatic representation while TRPES provides information about the electronic population of diabatic states.[45,52,53] However, an approximate comparison is feasible since a well-defined correspondence between adiabatic and diabatic states can be established for most surface-hopping trajectories of the pyrimidine bases.

Uracil. *Potential Energy Surfaces.* Uracil has the simplest geometrical and electronic structure of the molecules investigated in this paper. In agreement with previous experimental[54] and theoretical[5,17] findings, the ground-state equilibrium geometry of uracil is planar at the OM2 level. At this geometry the

Photoinduced Nonadiabatic Dynamics of Pyrimidine Nucleobases

*J. Phys. Chem. B, Vol. xxx, No. xx, XXXX* **C**

Figure 2. OM2 optimized structures (energy minima and conical intersections) and corresponding electronic energies (eV) of the low-lying states for uracil.
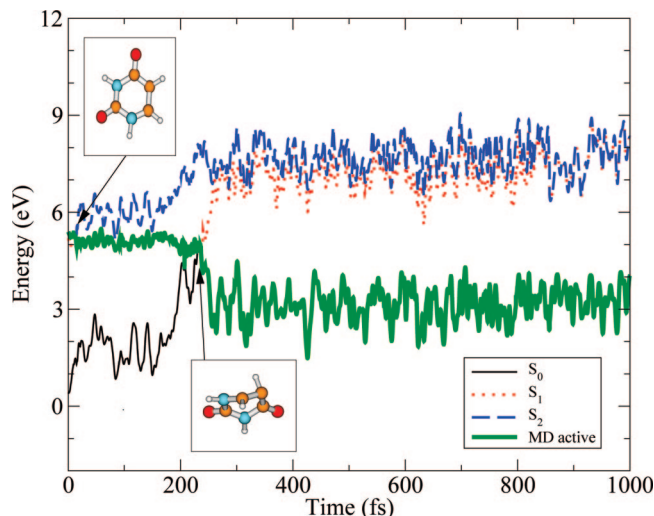

Figure 3. Potential energies sampled by a typical surface-hopping trajectory of uracil. The energy of the state on which the system is propagated is indicated in bold. The insets show molecular structures at hopping points.

first excited state (S_1) is the dark $n\pi^*$ state with a vertical excitation energy of 4.42 eV (see Figure 2). The second electronic state (S_2) with an energy of 4.96 eV is of $\pi\pi^*$ character, and because of its large oscillator strength it is responsible for the strong UV absorption of uracil. Computed excitation energies are consistent with experiments where an excitation energy of about 5.1 eV is measured for the $\pi\pi^*$ state[3,4] and are in good agreement with CASPT2 studies reporting excitation energies of 4.54 and 5.00 eV for the $n\pi^*$ and $\pi\pi^*$ state, respectively.[5,27]

The optimized geometry of the $n\pi^*$ state is planar at the OM2 level but shows small distortions in high-level calculations.[7,17] This small deficiency is possibly related to the lack of polarization functions in the OM2 basis set.[55] Except for this small difference the OM2 method yields a good description of the $n\pi^*$ equilibrium geometry. Going from the ground state to the $n\pi^*$-state minimum, the main geometrical changes observed at the OM2 level are the elongation of the C4−O4 and C5−C6 bonds by 0.08 and 0.03 Å, respectively, and the simultaneous shortening of the C4−C5 bond by 0.06 Å. Qualitatively similar (but larger) geometrical changes of 0.14, 0.07, and 0.10 Å are found at the MRCI level.[17] At the optimized geometry of the $n\pi^*$ state, the ground state is destabilized by 0.40 eV and the $n\pi^*$ state is stabilized by 0.37 eV, while the energy of the $\pi\pi^*$ state remains unchanged (see Figure 2). These trends are compatible with DFT/MRCI results, where the corresponding energy changes are 0.59, −0.65, and −0.27 eV, respectively.[7]

Unconstrained geometry optimization of the S_2 state starting from the ground-state equilibrium structure leads directly to the S_1−S_2 conical intersection connecting the $\pi\pi^*$ and the $n\pi^*$ states (CI_{u12} conical intersection) in analogy to ab initio studies at the MRCI, CC2, CASSCF(14,10), and MS-CASPT2(12,9) levels.[17,26,27,34] This intersection is located at 4.60 eV, between the vertical excitation energies of the $n\pi^*$ and $\pi\pi^*$ states (see Figure 2). The geometry of the CI_{u12} conical intersection is planar. Compared with the ground-state geometry, the N3−C4 and C5−C6 bond distances are increased by 0.04 and 0.12 Å, respectively, and the C2−N3, C4−C5, and C6−N1 bond lengths are reduced by 0.03, 0.06, and 0.04 Å, respectively. Comparable geometry changes are obtained in MRCI calculations[17] when planarity is imposed. However, if the planarity constraints are relaxed, the MRCI calculations show that small out-of-plane distortions yield a further stabilization of the CI_{u12} structure (by 0.35 eV).
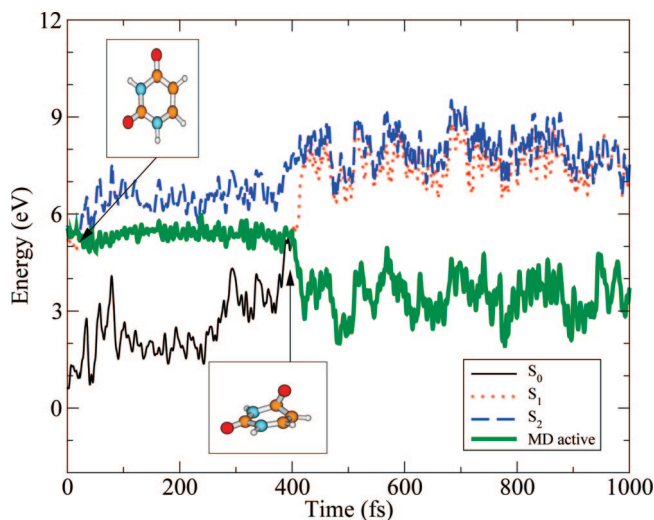
There are two important S_0−S_1 conical intersections in uracil. A large out-of-plane displacement of the H5 atom characterizes the S_0−S_1 conical intersection at 3.86 eV ($CI_{u01\alpha}$, see Figure 2) that connects the ground state and the $\pi\pi^*$ state. At the $CI_{u01\alpha}$ conical intersection, the C5−H5 bond is almost perpendicular to the ring plane with a dihedral angle δ(H5−C5−C6−C4) = 118°. Both the energy and the structure of this conical intersection are consistent with previous CASPT2 results[27] in which the $CI_{u01\alpha}$ conical intersection is located at 3.9 eV and the dihedral angle δ(H5−C5−C6−C4) is 114°.

A reduction of the S_0−S_1 energy gap is also induced by an out-of-plane displacement of the O4 atom. This distortion leads to a second S_0−S_1 conical intersection ($CI_{u01\beta}$) at 4.36 eV, which involves the ground state and the $n\pi^*$ state (see Figure 2). At the $CI_{u01\beta}$ conical intersection, the C4−O4 bond is almost perpendicular to the ring; the corresponding dihedral angle δ(C2−N3−C4−O4) is −87°, and the ring is somewhat distorted with a dihedral angle δ(C4−C5−C6−N1) of 24°.

Nonadiabatic Dynamics. After vertical excitation into the S_2 state ($\pi\pi^*$), an ultrafast $S_2 \rightarrow S_1$ decay takes place. Within 70 fs, the population of the S_2 state is completely transferred to the S_1 state. Afterward, a monotonic rise in the occupation of the S_0 state is observed, which indicates a slow $S_1 \rightarrow S_0$ population transfer. After 1.5 ps, more than 90% of the trajectories are in the S_0 state, and the internal conversion is essentially complete.

To elucidate the role of different conical intersections in the nonadiabatic dynamics of uracil and to determine the possible decay paths, a detailed analysis of the individual trajectories is needed. We show a typical uracil surface-hopping trajectory in Figure 3. Starting in the S_2 state, the molecule follows a downhill path and immediately approaches the CI_{u12} conical intersection, since this conical intersection is located very close to the Franck−Condon region. The strong $\pi\pi^*$/$n\pi^*$ electronic character mixing at the CI_{u12} conical intersection induces the hopping from the S_2 to the S_1 state. After the hopping the motion continues on the S_1 potential energy surface, until a S_0−S_1 conical intersection is accessed and internal conversion to the S_0 state occurs. For most trajectories, when the $S_1 \rightarrow S_0$ hopping occurs, the molecular geometry is characterized by a strong out-of-plane displacement of the O4 atom, and it can therefore be identified as the $CI_{u01\beta}$ conical intersection. Since this conical

Figure 4. Potential energies sampled by a surface-hopping trajectory of uracil passing through the CI$_{u01\alpha}$ conical intersection. The energy of state on which the system is propagated is indicated in bold. The insets show molecular structures at hopping points.
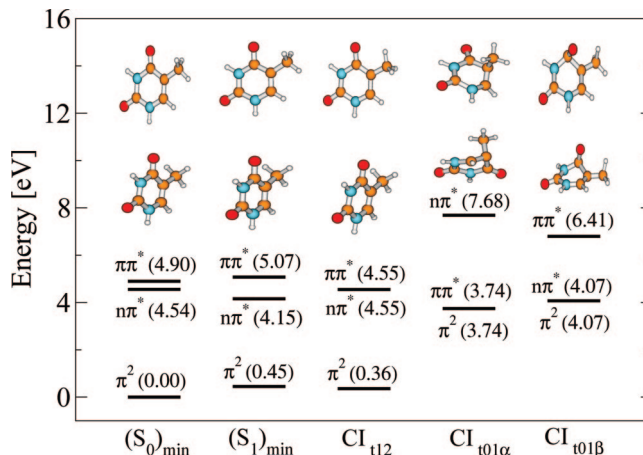

Figure 5. OM2 optimized structures (energy minima and conical intersections) and corresponding electronic energies (eV) of the low-lying states for thymine.

intersection connects the nπ* state with the ground state, such trajectories describe a two-step $\pi\pi$* → nπ* → gs decay.

A small number of trajectories (∼15%) follow a different nonadiabatic decay path (see Figure 4). The first part of the dynamics is similar to other trajectories, but after the S$_2$→ S$_1$ hopping at the CI$_{u12}$ conical intersection, the system leaves the interaction region with $\pi\pi$* electronic character. The dynamics then evolves toward the CI$_{u01\alpha}$ conical intersection and here the hopping to ground state occurs. Since this conical intersection connects the $\pi\pi$* state with the ground state, a state with nπ* character is not involved in this case. Therefore, although these trajectories show a two-step decay in the adiabatic representation, they describe in fact a direct $\pi\pi$* → gs decay. This direct $\pi\pi$* → gs decay is normally faster than the two-step $\pi\pi$* → nπ* → gs decay, but since only a few trajectories follow this path its contribution to the overall relaxation dynamics of uracil is small.

Fitting the time-dependent occupation of adiabatic states with an exponential model,[38] two time constants are found for the decay of the average occupation of excited states: τ_{S2} = 21 fs and τ_{S1} = 570 fs. The computed decay times compare well with TRPES experiments, which report an ultrafast decay with time constant <50 fs and a second component with decay time 530 fs.[18]

Thymine. *Potential Energy Surfaces.* The molecular structure of thymine is very similar to that of uracil (Figure 1), and the same applies also to the electronic structure. The OM2 optimized ground-state geometry of thymine is of C_s symmetry. The two lowest excited states are the dark nπ* and the bright $\pi\pi$* state with energies of 4.54 and 4.90 eV, respectively (see Figure 5). The same ordering of the states is found at the CASPT2 level: 4.39 eV (nπ*) and 4.88 eV ($\pi\pi$*).[4,5,27]

The OM2 calculations also give a planar nπ* minimum-energy structure that differs from the ground-state structure mainly with regard to the C4−O4 and C4−C5 bonds that are elongated by 0.09 and shortened by 0.07 Å, respectively. These geometry changes upon excitation are in good agreement with CASSCF optimizations that yield bond length variations of 0.11 and −0.09 Å.[26] At the nπ* geometry, the ground state and the $\pi\pi$* state are shifted to higher energies by 0.45 and 0.17 eV, respectively, while the nπ* state energy is decreased by 0.39 eV (relative to the ground-state minimum, see Figure 5).

In analogy with uracil, an attempt to optimize the $\pi\pi$*-state geometry starting from the ground-state minimum-energy structure directly leads to the S$_1$−S$_2$ conical intersection (CI$_{t12}$) connecting the $\pi\pi$* and the nπ* states. The CI$_{t12}$ conical intersection is located at 4.55 eV and has a planar geometry which does not differ much from the ground-state equilibrium geometry, except for some elongation of the C4−O4 and C5−C6 bond lengths (0.02 and 0.09 Å, respectively) and a reduction of the C4−C5 bond length by 0.06 Å. Similar bond length variations are found in CASSCF and CASPT2 calculations,[30,31] which however also reported out-of-plane deformations.

We located two S$_1$−S$_0$ conical intersections of thymine, namely the CI$_{t01\alpha}$ conical intersection (connecting the $\pi\pi$* state and the ground state) and the CI$_{t01\beta}$ conical intersection (connecting the nπ* state and the ground state). The CI$_{t01\alpha}$ conical intersection is located at 3.74 eV (4.0 eV in CASPT2 calculations).[27] In this configuration the CH$_3$ group shows a strong out-of-plane displacement with a characteristic dihedral angle δ(N3−C4−C5−C′5) = 81°; smaller distortions are observed at the H6 and C4 atom sites with dihedral angles δ(C2−N1−C6−H6) = 143° and δ(C4−C5−C6−N1) = 58°. For comparison, the corresponding values of the dihedral angles at the CASSCF level are δ(N3−C4−C5−C′5) = 83°, δ(C2−N1−C6−H6) = 148° and δ(C4−C5−C6−N1) = 50°, respectively.[26]

At the CI$_{t01\beta}$ conical intersection, the O4−C4 bond is strongly bent out-of-plane [δ(C2−N3−C4−O4) = −68°], in good agreement with CASSCF findings.[26,27] The CI$_{t01\beta}$ conical intersection is located at 4.07 eV, about 0.3 eV higher than the CI$_{t01\alpha}$ conical intersection.

Nonadiabatic Dynamics. In thymine, as in uracil, the nonadiabatic dynamics is characterized by a very fast S$_2$ → S$_1$ decay, followed by a slower S$_1$ → S$_0$ decay. After photoexcitation into the S$_2$ state, the average occupation of the S$_2$ state rapidly decreases and a complete transfer of population to the S$_1$ state occurs within 50 fs. Thereafter, the average population of the S$_0$ state starts to increase due to S$_1$ → S$_0$ hopping, until after 1 ps almost all trajectories are in the S$_0$ state. The decay times of the average occupation of the S$_2$ and S$_1$ states are τ_{S2} = 17 fs and τ_{S1} = 420 fs, respectively. These numbers are compatible with TRPES experiments, where time constants of <50 and 490 fs have been deduced.[18]

A typical surface-hopping trajectory of thymine is shown in Figure 6. Soon after photoexcitation into the S$_2$ state ($\pi\pi$*) the CI$_{t12}$ conical-intersection region is reached and hopping to the
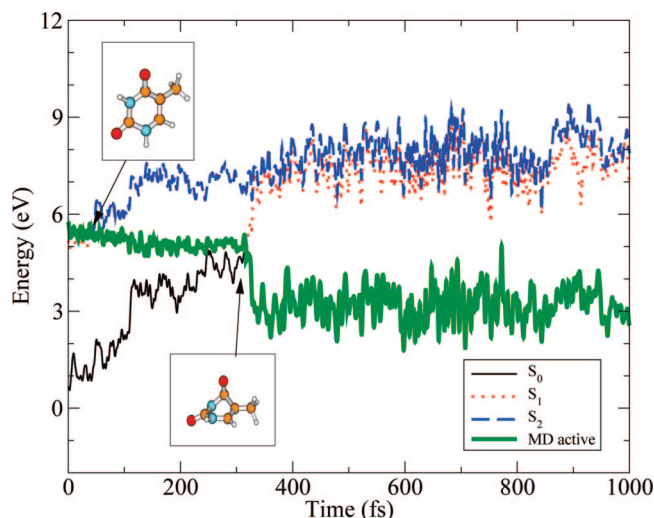
Figure 6. Potential energies sampled by a typical surface-hopping trajectory of thymine. The energy of the state on which the system is propagated is indicated in bold. The insets show molecular structures at hopping points.
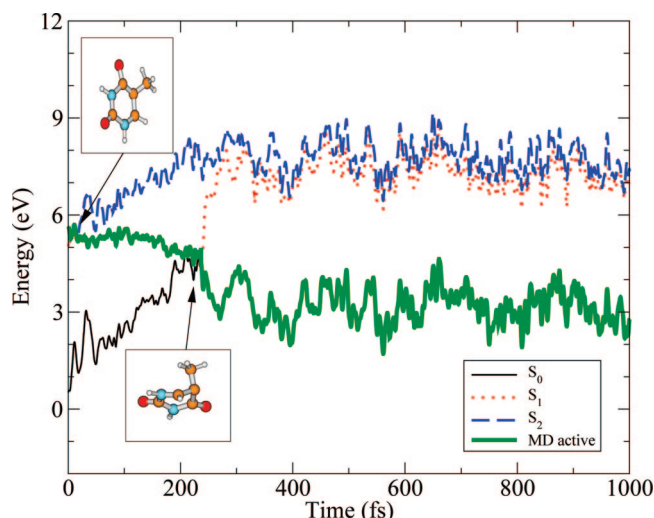
Figure 7. Potential energies sampled by a surface-hopping trajectory of thymine passing through the $CI_{t01\alpha}$ conical intersection. The energy of the state on which the system is propagated is indicated in bold. The insets show molecular structures at hopping points.

S_1 state occurs. After the hopping the electronic character of the S_1 state is mainly $n\pi^*$, and there is a pronounced out-of-plane motion of the O4 atom. Thus, the system evolves toward the $CI_{t01\beta}$ conical intersection and hops to the ground state. The electronic relaxation is described by a two-step $\pi\pi^* \rightarrow n\pi^* \rightarrow$ gs decay through the CI_{t12} and the $CI_{t01\beta}$ conical intersections with two distinctly different decay-time constants.

In a smaller number of trajectories (~18%) a different relaxation mechanism is observed (see Figure 7). In these trajectories the $S_2 \rightarrow S_1$ transition does not induce a change in the character of the electronically excited state, and the molecule thus retains $\pi\pi^*$ character after hopping. Therefore, the system is driven to the $CI_{t01\alpha}$ conical intersection. When the conical intersection is approached the hopping to the ground state finally occurs. In this case the relaxation dynamics is described by a direct $\pi\pi^* \rightarrow$ gs decay. As in the case of uracil, the direct $\pi\pi^*$ $\rightarrow$ gs decay mechanism is faster than the two-step $\pi\pi^* \rightarrow n\pi^*$ $\rightarrow$ gs decay mechanism, but gives only a minor contribution to the nonadiabatic dynamics of thymine.
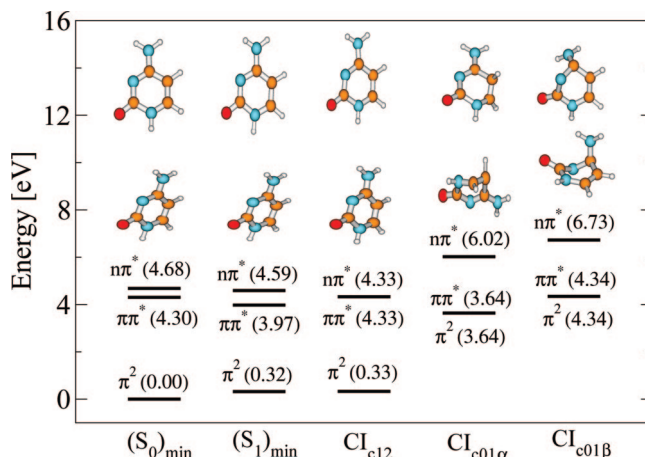
Figure 8. OM2 optimized structures (energy minima and conical intersections) and corresponding electronic energies (eV) of the low-lying states for cytosine.

Cytosine. *Potential Energy Surfaces.* The optimized ground-state geometry of cytosine is planar. The lowest excited state (S_1) is the bright $\pi\pi^*$ state, while the dark $n\pi^*$ state is the second excited state (S_2). This is the reverse of the order in uracil and thymine. At the OM2 level, the vertical excitation energies of the two states are 4.30 and 4.68 eV, respectively (see Figure 8). Similar values, 4.50 eV ($\pi\pi^*$) and 4.88 eV ($n\pi^*$), are found at the CASPT2 level.[11,27,56]

The $\pi\pi^*$ minimum-energy geometry differs from the equilibrium structure of the ground state mainly in having shorter C2−N3 and C4−C5 bonds (by 0.04 and 0.05 Å, respectively) and longer N3−C4 and C5−C6 bonds (by 0.07 and 0.05 Å, respectively). These changes are in qualitative agreement with those reported in previous ab initio calculations (0.11, 0.10, 0.13, and 0.10 Å, respectively).[11,19,27,29] At the $\pi\pi^*$ minimum, the S_0-S_1 energy gap is 3.65 eV, which is close to the 3.62 eV energy gap found at the CASPT2 level.[11,27]

Geometry optimization of the second excited state, starting from the ground-state minimum energy structure leads to the S_1-S_2 ($\pi\pi^*/n\pi^*$) conical intersection (CI_{c12}) at 4.33 eV. Its geometry is very similar to that of the ground-state minimum and thus lies within the Franck−Condon region.

Two S_1-S_0 conical intersections were located. The first one ($CI_{c01\alpha}$) at 3.64 eV connects the $\pi\pi^*$ and the ground state. Its geometry is characterized by a pronounced out-of-plane displacement of the H5 atom. The corresponding dihedral angle is δ (N3−C4−C5−H5) = −90°. In addition, ring deformations are observed, with dihedral angles δ(H6−C6−N1−C2) = −126° and δ(C4−C5−C6−N1) = −61°. A similar structure has been found at the CASSCF level with an energy of 3.6 eV (CASPT2) and dihedral angles δ(N3−C4−C5−H5) = −90°, δ(H6−C6−N1−C2) = −133° and δ(C4−C5−C6−N1) = −50°.[27]

The second S_1-S_0 conical intersection ($CI_{c01\beta}$) is located at 4.34 eV. Its energy is 0.37 eV higher than that of the $\pi\pi^*$ state at its minimum (0.43 eV at CASPT2 level)[11,27] and 0.04 eV higher than the energy of the $\pi\pi^*$ state at the ground-state minimum. At this intersection, the C4−N4 bond is almost perpendicular to the ring, as indicated by the dihedral angle δ(N4−C4−C5−C6) = −97°. There is also some displacement of the N3 atom, with the dihedral angle δ(C2−N3−C4−C5) = −62°. An S_1-S_0 conical intersection of this kind has also been found in CASSCF,[10,11,27] MRCI,[29] and DFT/MRCI[19] calculations, but there is no consensus on the electronic character of the electronic states involved; it has been described either as a $n\pi^*$/
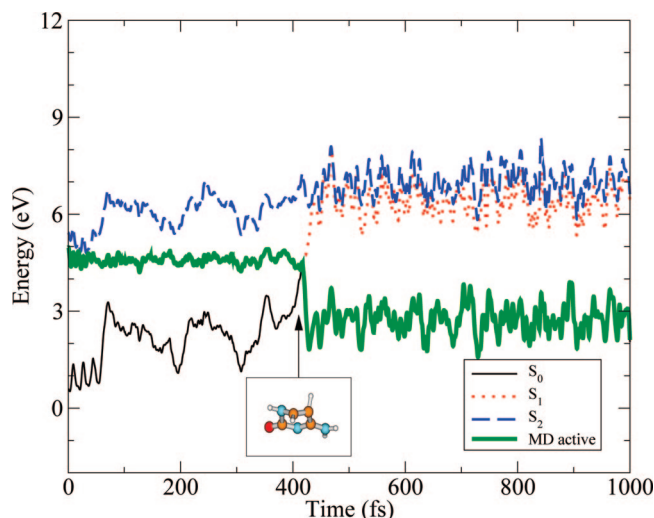
Figure 9. Potential energies sampled by a typical surface-hopping trajectory of cytosine starting in the S_1 state. The energy of the state on which the system is propagated is indicated in bold. The inset shows the molecular structure at the hopping point.

Figure 10. Potential energies sampled by a typical surface-hopping trajectory of cytosine starting in the S_2 state. The energy of the state on which the system is propagated is indicated in bold. The inset shows the molecular structure at the hopping point.

gs conical intersection[10,11,27] or as a $\pi\pi$*/gs conical intersection associated with a so-called "sofa" distortion.[29] In the present work, it is of $\pi\pi$*/gs type, but this turns out to be less relevant for our purposes since this intersection plays no role in our surface-hopping simulations of cytosine, presumably because of its high energy.
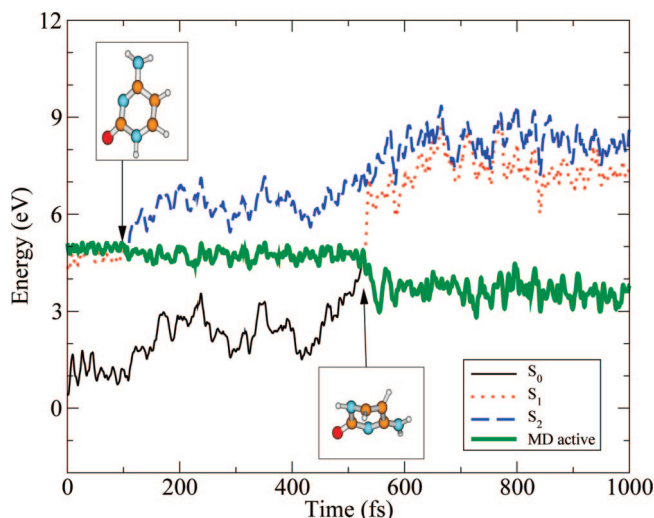
Nonadiabatic Dynamics. Unlike uracil and thymine, the optically active state of cytosine is the first excited state (S_1). Accordingly, all surface-hopping trajectories should start in the S_1 state. In this case only two electronic states are involved in the nonadiabatic dynamics and throughout the whole simulation the S_2 state remains unpopulated. The dynamics follows a direct $S_1 \rightarrow S_0$ ($\pi\pi$* $\rightarrow$ gs) decay path with a time constant of 350 fs. The hopping occurs at geometries characterized by a strong out-of-plane displacement of the H5 atom, indicating that the $CI_{c01\alpha}$ conical intersection is involved (see Figure 9).

The above description of the nonadiabatic dynamics of cytosine is however incomplete, since it neglects the role of the S_2 ($n\pi$*) state and cannot give any explanation for the ultrashort component observed in the TRPES spectra.[18] In fact, a proper treatment of the initial conditions of surface-hopping dynamics in cytosine needs to take into account that in the Franck–Condon region the S_1-S_2 energy gap is small. Hence, in many configurations in the vicinity of the ground-state minimum, the lowest two excited states are strongly mixed. Consequently, the vertical absorption of a photon during ground-state motion will induce transitions to both excited states, and trajectories starting in the S_2 state must be considered as well. A typical trajectory starting in the S_2 state is shown in Figure 10. In this case an ultrafast $S_2 \rightarrow S_1$ decay is observed with a time constant of 40 fs. After this, the dynamics follows a similar path as described above, and the internal conversion proceeds through a $S_1 \rightarrow S_0$ decay with a time constant of 513 fs.

The computed decay times of 40 fs ($S_2 \rightarrow S_1$) and 370 fs ($S_1 \rightarrow S_0$, average over both paths) compare reasonably well with the experimental observed time constants of <50 and 820 fs,[18] respectively, but the agreement is not as good as for uracil and thymine.

Discussion

We first address common features as well as differences that emerge from the present study of the three pyrimidine nucleo-

bases. In each of these molecules the nonadiabatic dynamics following photoexcitation involves the three lowest singlet states which are connected by several conical intersections. The S_1-S_2 conical intersection is characterized by very small distortions and is located in close proximity to the Franck–Condon region. It is thus rapidly accessible after photoexcitation which gives rise to an ultrafast decay of the occupation of the S_2 state in all three molecules.

The excited states are connected to the ground state by at least two conical intersections. The first one ($CI_{01\alpha}$) is strongly distorted at the C5 atom, with the C5–R bond (where R = H5 for uracil and cytosine and R = C'5 for thymine) almost perpendicular to the ring. It links the $\pi\pi$* state to the ground state. The second conical intersection ($CI_{01\beta}$) is characterized by a large out-of-plane distortion at the C4 atom, with the C4–R bond (where R = O4 for uracil and thymine and R = N4 for cytosine) almost perpendicular to the ring. It connects the ground state with the $n\pi$* state in uracil and thymine and with the $\pi\pi$* state in cytosine. The $CI_{01\beta}$ conical intersection is the most important one for the internal conversion to the ground state in uracil and thymine, while it plays no role in the nonadiabatic dynamics of cytosine. The $CI_{01\alpha}$ conical intersection is essential for the nonradiative relaxation of cytosine and plays a secondary role in the internal conversion of uracil and thymine.

The main difference between uracil and thymine on one hand and cytosine on the other hand is the ordering of the two lowest excited states at the ground-state equilibrium geometry, where the bright $\pi\pi$* state is the second excited state in uracil and thymine, but the first one in cytosine. This different state ordering influences the starting occupation of adiabatic states used in the surface-hopping simulations. Furthermore, in cytosine there is a strong electronic mixing between the $\pi\pi$* and $n\pi$* states in configurations very close to the ground-state minimum because of the small S_2-S_1 energy gap. The $\pi\pi$* state has an energy minimum in cytosine, but not in uracil and thymine, consistent with the experimentally observed sharp vibronic spectra in cytosine as opposed to the broad spectra in uracil and thymine.[8]

Photoexcitation of uracil and thymine populates the bright S_2 ($\pi\pi$*) state. In the adiabatic representation, the nonradiative relaxation then proceeds by a $S_2 \rightarrow S_1 \rightarrow S_0$ mechanism with an ultrafast $S_2 \rightarrow S_1$ transition followed by a slower $S_1 \rightarrow S_0$

transition. In most trajectories ($\sim$85%) the $S_1 \rightarrow S_0$ transition occurs in the proximity of the $CI_{01\beta}$ conical intersection, therefore the dominant decay mechanism can be regarded as a two-step $\pi\pi^* \rightarrow n\pi^* \rightarrow$ gs process. Only a small contribution comes from trajectories passing through the $CI_{01\alpha}$ conical intersection in a fast direct $\pi\pi^* \rightarrow$ gs decay. On the other hand, for cytosine it is necessary to consider trajectories starting both in the S_1 ($\pi\pi^*$) state and in the S_2 ($n\pi^*$) state, because of the electronic mixing of these states in the Franck–Condon region. Trajectories starting in the S_1 state are dominant. They follow a direct $S_1 \rightarrow S_0$ path, while those starting in the S_2 state show instead a two-step $S_2 \rightarrow S_1 \rightarrow S_0$ decay with an ultrafast $S_2 \rightarrow S_1$ transition followed by a slower $S_1 \rightarrow S_0$ transition.

We now turn to a comparison with the results from TRPES experiments which report a double exponential decay having an ultrafast component with a lifetime of <50 fs in each molecule and a second subpicosecond component with lifetimes of 530, 490, and 820 fs in uracil, thymine, and cytosine, respectively.[18] The geometries explored in our surface-hopping trajectories are such that ionization by the probe pulse used experimentally (6.2 eV) is generally possible for both the S_1 and S_2 state, that is, the corresponding cations are energetically accessible by one-photon ionization. Assuming the same photoionization cross section for both states, we can relate the time-dependent average populations of these states (see Figures S1–S3 of the Supporting Information) to the experimentally deduced decay times.[18] Fitting our data for uracil, thymine, and cytosine with an exponential model[38] yields time constants of 21, 17, and 40 fs for the ultrafast $S_2 \rightarrow S_1$ decay and 570, 420, and 370 fs for the slower $S_1 \rightarrow S_0$ transition, respectively, which are reasonably close to the experimentally deduced values (see above). The largest discrepancy is found for the second component in cytosine (370 versus 820 fs). In this case, the overall time constant for the $S_1 \rightarrow S_0$ decay is determined by the relative number of trajectories starting in the S_1 and S_2 states and by the computed decay times for the two pathways (350 and 513 fs, respectively). The average calculated decay time of 370 ps would increase if more trajectories were starting from the S_2 state (i.e., if the S_2-S_1 energy gap were smaller), but it would even then remain below the experimental value of 820 fs. In any event, considering all the approximation made, the overall agreement between the theoretical and experimental results is better than we would have expected.

As mentioned in the introduction, there is a recent AIMS study of excited-state dynamics in uracil and thymine[30,31] that arrives at a qualitatively different mechanistic picture, which is distinct from the one in our present surface-hopping calculations and also from proposals that are based on static ab initio explorations of the relevant excited-state potential energy surfaces.[17,21,26,27,34] This AIMS study attributes the ultrafast decay of the photoelectron signal in TRPES experiments[18] not to electronic quenching, but to relaxation within the S_2 state toward structures that can no longer be ionized by the probe pulse (6.2 eV). The 500 fs AIMS simulations explore the motion on the S_2 surface toward and around a true minimum with biradical character without reaching a conical intersection that would allow for surface crossing. The AIMS dynamics has been done at the SA-3-CASSCF(8,6)/6-31G* level with additional static calculations at the SA-5-MS-CASPT2(8,7)/6-31G* level that support the existence of the S_2 minimum and rationalize the outcome of the AIMS simulations in terms of suitable relaxation paths. The existence and dynamic accessibility of the S_2 minimum is obviously of crucial importance for the reported AIMS dynamics. We note that there is no consensus on this

issue in the literature,[17,26,27,34] and hence there is a need for further high-level calculations to settle this point. As pointed out before,[31] it should also be possible to discriminate experimentally between the relaxation mechanism suggested in the AIMS study and the quenching mechanism found in the present surface-hopping study, by using probe pulses of higher energy: this should affect the experimental results strongly only if the relaxation mechanism operates (not in the case of electronic quenching). We hope that the conflicting theoretical results discussed above will trigger such experimental work.

Finally, we address the accuracy of excited-state nonadiabatic dynamics. It is evident that such calculations are challenging and require compromises between computational effort and accuracy. None of the presently feasible approaches is accurate enough to provide definitive results for medium-size molecules. Ab initio CASSCF dynamics calculations are often still restricted to rather short simulation times, and they suffer from the neglect of dynamic correlation which may affect different states to different extent and may thus lead to an unbalanced treatment. Semiempirical dynamics calculations with the currently chosen OM2/MRCI surface-hopping approach are much more efficient and allow the computation of many long trajectories, but being semiempirical their intrinsic accuracy is limited and must always be validated carefully against high-level ab initio results, for example, from CASPT2 calculations.[27,34,57] If this can be done successfully, OM2/MRCI nonadiabatic dynamics may offer mechanistic insights that are not obvious from static calculations.

In the case of the three pyrimidine bases, we have shown (see Results) that OM2/MRCI reproduces the optimized geometries and relative energies from ab initio calculations reasonably well, both for excited-state minima and conical intersections. Taking uracil as an example, recent CASPT2 calculations[27] place the bright S_2 ($\pi\pi^*$) state at 5.02 eV after vertical excitation and document a barrierless downhill path from the Franck–Condon geometry to the $CI_{01\alpha}$ conical intersection with the ground state at 3.9 eV; this relaxation path is viewed as the origin of the ultrafast initial deactivation.[27] Similarly, OM2/MRCI gives a barrierless downhill path from the Franck–Condon geometry of the S_2 ($\pi\pi^*$) state at 4.96 eV to the analogous conical intersection at 3.86 eV. However, the OM2/MRCI surface-hopping simulations favor a stepwise relaxation with an ultrafast $S_2 \rightarrow S_1$ transition followed by a slower $S_1 \rightarrow S_0$ transition and not the direct decay expected from static calculations,[27] because the nonadiabatic coupling of the S_2 ($\pi\pi^*$) state to the nearby S_1 ($n\pi^*$) state is strong enough to prefer the stepwise over the direct electronic deexcitation (85% versus 15% of the trajectories). In this case the explicit consideration of dynamics thus modifies and refines the static view of the relaxation mechanism.

Conclusions

The electronic structure and nonadiabatic dynamics of the three pyrimidine nucleobases, uracil, thymine, and cytosine, have been studied using the semiempirical OM2 method with GUGA configuration interaction.

The potential energy surfaces of the ground state and the two lowest singlet excited states of these molecules have been characterized by locating the relevant energy minima and conical intersections and by computing excitation energies at the optimized geometries. The computed structures are generally rather similar, in particular also for the different types of conical intersections. Uracil and thymine have analogous energy spectra, with the $n\pi^*$ state below the $\pi\pi^*$ state, whereas cytosine has the opposite state order and also a different electronic character of the $CI_{01\beta}$ conical intersection.

According to the OM2-GUGACI surface-hopping molecular dynamics calculations, the relaxation dynamics of uracil and thymine follows a $S_2 \rightarrow S_1 \rightarrow S_0$ mechanism with a dominant two-step $\pi\pi^* \rightarrow n\pi^* \rightarrow$ gs decay and a small contribution from a direct $\pi\pi^* \rightarrow$ gs decay. In cytosine, the direct $S_1 \rightarrow S_0$ pathway is most important with a smaller contribution from trajectories representing an $S_2 \rightarrow S_1 \rightarrow S_0$ pathway, so that the overall $S_1 \rightarrow S_0$ decay time is obtained as a weighted average of these two processes. In all three molecules, both lowest excited singlet states are important for the nonadiabatic dynamics.

The OM2-GUGACI potential surfaces for the three pyrimidine bases are in reasonable agreement with the available data from published static ab initio studies. The present results of the surface-hopping calculations compare well with the decay times deduced from time-resolved photoelectron spectroscopy, especially for uracil and thymine. In the case of cytosine, the decay time of the S_1 state is underestimated by a factor of about 2 relative to the TRPES measurement.

In an overall assessment, the OM2-GUGACI method appears to provide a reasonable description of the photoinduced non-radiative relaxation of the pyrimidine bases uracil, thymine, and cytosine, as well as in the case of adenine studied previously.[38] The method is efficient and practical as can be seen from the fact that we have easily computed for each molecule around 100 surface hopping trajectories (1.6 ps each). We have implemented this approach not only in our semiempirical MNDO program (used here), but also in the ChemShell software for combined quantum mechanical/molecular mechanical (QM/MM) calculations which enables analogous studies of complex systems in a QM/MM context. Applications of this kind are in progress.

Supporting Information Available: Energies of electronic states at different geometries, Cartesian and internal coordinates of the three molecules at energy minima and conical intersections, and plots of the average occupation of the lowest adiabatic states as function of time. This material is available free of charge via the Internet at http://pubs.acs.org.

References and Notes

(1) Callis, P. R. *Annu. Rev. Phys. Chem.* **1983**, *34*, 329.

(2) Crespo-Hernández, C. E.; Cohen, B.; Hare, P. M.; Kohler, B. *Chem. Rev.* **2004**, *104*, 1977.

(3) Saigusa, H. *J. Photochem. Photobiol. C* **2006**, *7*, 197.

(4) Shukla, M. K.; Leszczynski, J. *J. Biomol. Struct. Dyn.* **2007**, *25*, 93.

(5) Lorentzon, J.; Fülscher, M. P.; Roos, B. O. *J. Am. Chem. Soc.* **1995**, *117*, 9265.

(6) Shukla, M. K.; Mishra, P. C. *Chem. Phys.* **1999**, *240*, 319.

(7) Marian, C. M.; Schneider, F.; Kleinschmidt, M.; Tatchen, J. *Eur. Phys. J. D* **2002**, *20*, 357.

(8) Nir, E.; Müller, M.; Grace, L. I.; de Vries, M. S. *Chem. Phys. Lett.* **2002**, *355*, 59.

(9) Kang, H.; Lee, K. T.; Jung, B.; Ko, Y. J.; Kim, S. K. *J. Am. Chem. Soc.* **2002**, *124*, 12958.

(10) Ismail, N.; Blancafort, L.; Olivucci, M.; Kohler, B.; Robb, M. A. *J. Am. Chem. Soc.* **2002**, *124*, 6818.

(11) Merchán, M.; Serrano-Andrés, L. *J. Am. Chem. Soc.* **2003**, *125*, 8108..

(12) He, Y.; Wu, C.; Kong, W. *J. Phys. Chem. A* **2003**, *107*, 5145.

(13) Malone, R. J.; Miller, A. M.; Kohler, B. *Photochem. Photobiol.* **2003**, *77*, 158.

(14) Cohen, B.; Crespo-Hernández, C. E.; Kohler, B. *Faraday Discuss.* **2004**, *127*, 137.

(15) He, Y.; Wu, C.; Kong, W. *J. Phys. Chem. A* **2004**, *108*, 943.

(16) Blancafort, L.; Robb, M. A. *J. Phys. Chem. A* **2004**, *108*, 10609.

(17) Matsika, S. *J. Phys. Chem. A* **2004**, *108*, 7584.

(18) Ullrich, S.; Schultz, T.; Zgierski, M. Z.; Stolow, A. *Phys. Chem. Chem. Phys.* **2004**, *6*, 2796.

(19) Tomic, K.; Tatchen, J.; Marian, C. M. *J. Phys. Chem. A* **2005**, *109*, 8410.

(20) Matsika, S. *J. Phys. Chem. A* **2005**, *109*, 7538.

(21) Zgierski, M. Z.; Patchkovskii, S.; Fujiwara, T.; Lim, E. C. *J. Phys. Chem. A* **2005**, *109*, 9384.

(22) Zgierski, M. Z.; Patchkovskii, S.; Lim, E. C. *J. Chem. Phys.* **2005**, *123*, 081101.

(23) Samoylova, E.; Lippert, H.; Ullrich, S.; Hertel, I. V.; Radloff, W.; Schultz, T. *J. Am. Chem. Soc.* **2005**, *127*, 1782.

(24) Gustavsson, T.; Bányász, A.; Lazzarotto, E.; Markovitsi, D.; Scalmani, G.; Frisch, M.; Barone, V.; Improtav, R. *J. Am. Chem. Soc.* **2006**, *128*, 607.

(25) Canuel, C.; Mons, M.; Piuzzi, F.; Tardivel, B.; Dimicoli, I.; Elhanine, M. *J. Chem. Phys.* **2005**, *122*, 074316.

(26) Perun, S.; Sobolewski, A. L.; Domcke, W. *J. Phys. Chem. A* **2006**, *110*, 13238.

(27) Merchán, M.; González-Luque, R.; Climent, T.; Serrano-Andrés, L.; Rodrígues, E.; Reguero, M.; Peláez, D. *J. Phys. Chem. B* **2006**, *110*, 26471.

(28) Gustavsson, T.; Sarkar, N.; Lazzarotto, E.; Markovitsi, D.; Improta, R. *Chem. Phys. Lett.* **2006**, *429*, 551.

(29) Kistler, K. A.; Matsika, S. *J. Phys. Chem. A* **2007**, *111*, 2650.

(30) Hudock, H. R.; Levine, B. G.; Thompson, A. L.; Martínez, T. J. *AIP Conf. Proc.* **2007**, *963*, 219.

(31) Hudock, H. R.; Levine, B. G.; Thompson, A. L.; Satzger, H.; Townsend, D.; Gador, N.; Ullrich, S.; Stolow, A.; Martínez, T. J. *J. Phys. Chem. A* **2007**, *111*, 8500.

(32) Zgierski, M. Z.; Fujiwara, T.; Lim, E. C. *Chem. Phys. Lett.* **2008**, *463*, 289.

(33) Nieber, H.; Doltsinis, N. L. *Chem. Phys.* **2008**, *347*, 405.

(34) Mercier, F.; Santoro, F.; Reguero, M.; Improta, R. *J. Phys. Chem. B* **2008**, *112*, 10769.

(35) Kwok, W.-M.; Ma, C.; Lee Phillips, D. *J. Am. Chem. Soc.* **2008**, *130*, 5131.

(36) Zechmann, G.; Barbatti, M. *J. Phys. Chem. A* **2008**, *112*, 8273.

(37) Sobolewski, A. L; Domcke, W.; Dedonder-Lardeux, C.; Jouvet, C. *Phys. Chem. Chem. Phys.* **2002**, *4* (2002), 1093.

(38) Fabiano, E.; Thiel, W. *J. Phys. Chem. A* **2008**, *112*, 6859.

(39) Weber, W. Ph.D. Thesis, Universität Zürich, Zürich, Switzerland, 1996.

(40) Weber, W.; Thiel, W. *Theor. Chem. Acc.* **2000**, *103*, 495.

(41) Koslowski, A.; Beck, M. E.; Thiel, W. *J. Comput. Chem.* **2003**, *24*, 714.

(42) Tully, J. C. *J. Chem. Phys.* **1990**, *93*, 1061.

(43) Hammes-Schiffer, S.; Tully, J. C. *J. Chem. Phys.* **1994**, *101*, 4657.

(44) Thiel, W. *MNDO program*, version 6.1; Mülheim an der Ruhr: Germany, 2007.

(45) Domcke, W. ; Yarkony, D. R. ; Köppel, H. *Conical Intersections: Electronic Structure, Dynamics and Spectroscopy*; World Scientific: Singapore, 2004.

(46) Keal, T. W.; Koslowski, A.; Thiel, W. *Theor. Chem. Acc.* **2007**, *118*, 837.

(47) Satger, H.; Townsend, D.; Zgierski, M. Z.; Patchkovskii, S.; Ullrich, S.; Stolow, A. *Proc. Natl. Acad. Sci. U.S.A.* **2006**, *103*, 10196.

(48) Nix, M. G. D.; Devine, A. L.; Cronin, B.; Ashfold, M. N. R. *J. Chem. Phys.* **2007**, *126*, 124312.

(49) Fabiano, E.; Keal, T. W.; Thiel, W. *Chem. Phys.* **2008**, *349*, 334.

(50) Barbatti, M.; Granucci, G.; Persico, M.; Ruckenbauer, M.; Vazdar, M.; Eckert-Maksić, M.; Lischka, H. *J. Photochem. Photobiol. A* **2007**, *190*, 228.

(51) Swope, W. C.; Andersen, H. C.; Berens, P. H.; Wilson, K. R. *J. Chem. Phys.* **1982**, *76*, 637.

(52) Seel, M.; Domcke, W. *J. Chem. Phys.* **1991**, *95*, 7806.

(53) Stolow, A. *Annu. Rev. Phys. Chem.* **2003**, *54*, 89.

(54) Taylor, R.; Kennard, O. *J. Am. Chem. Soc.* **1982**, *104*, 3209.

(55) Broo, A. *J. Phys. Chem.* **1998**, *102*, 526.

(56) Fülscher, M. P.; Roos, B. O. *J. Am. Chem. Soc.* **1995**, *117*, 2089.

(57) Schreiber, M.; Silva-Junior, M. R.; Sauer, S. P. A.; Thiel, W. *J. Chem. Phys.* **2008**, *128*, 134110.